Volume 72, Number 1
January 1, 2008

ELSEVIER

Geochimica et Cosmochimica Acta

JOURNAL OF THE GEOCHEMICAL SOCIETY
AND THE METEORITICAL SOCIETY

Continued on outside back cover

Available online at www.sciencedirect.com
ScienceDirect
Geochimica et Cosmochimica Acta 72 (2008) 19–35
Geochimica et Cosmochimica Acta
www.elsevier.com/locate/gca

Turnover of oxygen and hydrogen isotopes in the body water, CO_2, hair, and enamel of a small mammal

David W. Podlesak [a,*], Ann-Marie Torregrossa [a], James R. Ehleringer [a], M. Denise Dearing [a], Benjamin H. Passey [b], Thure E. Cerling [a,b]

[a] Department of Biology, University of Utah, Salt Lake City, UT 84112-0840, USA
[b] Department of Geology and Geophysics, University of Utah, Salt Lake City, UT 84112-0111, USA

Received 17 April 2007; accepted in revised form 4 October 2007; available online 12 October 2007

Abstract

Oxygen and hydrogen isotope signatures of animal tissues are strongly correlated with the isotope signature of local precipitation and as a result, isotope signatures of tissues are commonly used to study resource utilization and migration in animals and to reconstruct climate. To better understand the mechanisms behind these correlations, we manipulated the isotope composition of the drinking water and food supplied to captive woodrats to quantify the relationships between drinking water (δ_{dw}), body water (δ_{bw}), and tissue (δ_t). Woodrats were fed an isotopically constant food but were supplied with isotopically depleted or enriched water. Some animals were switched between these waters, allowing simultaneous determination of body water turnover, isotope change recorded in teeth and hair, and fractional contributions of atmospheric O_2, drinking water, and food to the oxygen and hydrogen budgets of the animals. The half-life of the body water turnover was 3–6 days. A mass balance model estimated that drinking water, atmospheric O_2, and food were responsible for 56%, 30%, and 15% of the oxygen in the body water, respectively. Drinking water and food were responsible for 71% and 29% of the hydrogen in the body water, respectively. Published generalized models for lab rats and humans accurately estimated δ_{bw}, as did an updated version of a specific model for woodrats. The change in drinking water was clearly recorded in hair and tooth enamel, and multiple-pool and tooth enamel forward models closely predicted these changes in hair and enamel, respectively. Oxygen and hydrogen atoms in the drinking water strongly influence the composition of the body water and tissues such as hair and tooth enamel; however, food and atmospheric O_2 also contribute oxygen and/or hydrogen atoms to tissue. Controlled experiments allow researchers to validate models that estimate δ_t based on δ_{dw} and so will increase the reliability of estimates of resource utilization and climate reconstruction.

1. INTRODUCTION

Stable isotopes of oxygen and hydrogen are increasingly used as tracers to study modern and ancient systems (Hoppe et al., 2004; Bowen et al., 2005b). Ecologists have used oxygen and hydrogen isotopes in blood, hair and feathers to elucidate patterns of resource utilization and identify paths of migration (Hobson and Wassenaar, 1997; Wolf and Martinez del Rio, 2003; Hobson, 2005). Similarly, oxygen isotopes in bone and teeth have been used to reconstruct climate and paleoecological conditions (Ayliffe and Chivas, 1990; Fricke et al., 1998; Hoppe, 2006). In general, the oxygen and hydrogen isotopic ratios in animal tissues (δ_t) are strongly correlated with the isotopic composition of local precipitation (δ_p) and δ_p varies inversely with latitude and elevation (Dansgaard, 1964; Bowen and Revenaugh, 2003). As a result, δ_t can been used to predict the location of origin for samples (Bowen et al., 2005b; Hobson, 2005). Similarly, if the location of origin is known, $\delta^{18}O$ values of tooth enamel or bone collagen have been used to reconstruct ancient precipitation patterns (Fricke et al., 1998; Hoppe, 2006).

Overall, the correlation between δ_p and δ_t is robust. However, regression equations between δD_p and δD_t are

* Corresponding author.
E-mail address: podlesak@biology.utah.edu (D.W. Podlesak).

0016-7037/$ - see front matter © 2007 Elsevier Ltd. All rights reserved.
doi:10.1016/j.gca.2007.10.003

rarely at unity, and $\delta^{18}O_p$ and $\delta^{18}O_t$ are never at unity because of the incorporation of molecular O_2 into the body water and subsequently into tissue (Kohn, 1996; Bowen et al., 2005b; Lott and Smith, 2006). In addition, the body water (δ_{bw}) of animals is influenced by drinking water (i.e., local precipitation), diet, climate, and physiology (Luz and Kolodny, 1985; Bryant et al., 1996; Kohn, 1996; McKechnie et al., 2004). Tissues such as hair and feathers are greatly influenced by the composition of body water (Hobson et al., 1999; Sharp et al., 2003). Consequently, the ability to use $\delta^{18}O_t$ and δD_t to study the ecology of modern animals and to reconstruct climate requires an understanding of the various inputs and mechanisms that influence δ_{bw}, and subsequently δ_t.

Predictive models based on the daily flux of oxygen and hydrogen have been developed that estimate δ_{bw} for animals (Luz et al., 1984; Schoeller et al., 1986a; Bryant et al., 1996; Kohn, 1996). Selected models include climatic and physiological parameters and also include estimates of δ_t, specifically $\delta^{18}O$ of phosphate (Luz et al., 1984; Schoeller et al., 1986a; Bryant et al., 1996; Kohn, 1996). However, there are no similar models for δD and $\delta^{18}O$ of hair. There have been few studies designed to test the various body water models and to detail the relationships between drinking water, body water, hair, and tooth enamel. Likewise, there has been limited research on the rate of change in the isotopic composition of body water, hair, and tooth enamel after a change in location or a change in resource use by an animal.

In this study, we controlled the isotope composition of drinking water (δ_{dw}) supplied to two species of woodrats to quantify the relationships between δ_{dw} and δ_{bw}, and to quantify the relationships between body water and breath CO_2, hair, and tooth enamel. We also switched animals between waters that were isotopically depleted and isotopically enriched. All animals were exposed to the same environmental conditions, and the macronutrient and isotopic composition of the diet were held constant. The controlled conditions of this experiment allowed us to evaluate published body water models that predict δ_{bw} based on δ values of drinking water (δ_{dw}). We used measured δ_{bw} values combined with measured δ values of food (δ_{fd}) to create a mass balance model that estimates the proportion of oxygen and hydrogen atoms in the body water of the woodrats that are from drinking water, food, and atmospheric O_2. We used the reaction progress method to describe the turnover of the body water and hair in the woodrats, and we used a multiple-pool model to describe the flow of oxygen and hydrogen atoms into hair. Lastly, this experimental design allowed us to evaluate a forward modeling technique that predicts $\delta^{18}O$ of tooth enamel after a change in drinking water for a small rodent.

2. MATERIALS AND METHODS

2.1. Stable isotopes

Stable isotope ratios are reported in δ-notation as parts per thousand (‰) deviations from an international standard according to the equation:

$$\delta_A = (R_A/R_{STD} - 1) * 1000 \quad (1)$$

where R_A is the corresponding ratio ($^2H/^1H$, $^{13}C/^{12}C$, $^{18}O/^{16}O$) of the sample and R_{STD} is the isotope ratio of the standard. Isotope fractionation is the difference between two phases in equilibrium:

$$\alpha_{AB} = R_A/R_B = (1000 + \delta_A)/(1000 + \delta_B) \quad (2)$$

and isotope enrichment is

$$\varepsilon_{AB} = (\alpha_{AB} - 1) * 1000 \quad (3)$$

We use α_{AB} and ε_{AB} for isotope fractionation at equilibrium and α^*_{AB} and ε^*_{AB} for isotope difference (non-equilibrium).

See Table 1 for key to notation used in the text, models, tables, and figures.

2.2. Experimental design

To accurately test existing models that predict δD and $\delta^{18}O$ of body water and hair, and $\delta^{18}O$ of tooth enamel, we had to quantify the rate of turnover of oxygen and hydrogen in the body water of a mammal. We chose to study the flow of oxygen and hydrogen atoms from drinking water into tissue for a small rodent because rodent hair and teeth are commonly found in midden mounds and have the potential to be used as a tool to trace resource use for modern and ancient systems as well as reconstruct ancient climate. We controlled the isotopic composition of the drinking water and food supplied to two species of woodrats; *Neotoma cinerea* and *N. stephensi*. *N. cinerea* were trapped in Summit County, Utah and *N. stephensi* were trapped in Coconino County, AZ. All animals were housed at the University of Utah's animal facilities in individual cages in the same room with a constant light cycle (12 h dark:12 h light) and temperature (25 °C). Prior to the experiment, the 7 *N. cinerea* had been in captivity for >2 years and the 10 *N. stephensi* for 6 months. The woodrats had been eating the same food ($\delta D = -109 \pm 4$‰; $\delta^{18}O = 24.0 \pm 0.2$‰) and drinking relatively isotopically depleted water.

First, we switched 5 *N. cinerea* and 7 *N. stephensi* from the depleted water ($\delta D = -121 \pm 1$‰; $\delta^{18}O = -16.1 \pm 0.2$‰) to enriched drinking water ($\delta D = 339 \pm 2$‰; $\delta^{18}O = 15.0 \pm 0.2$‰) and the remaining 2 *N. cinerea* and 3 *N. stephensi* continued to drink depleted water (control groups). The isotopic composition of the water was 31‰ and 460‰ different in the amount of ^{18}O and D, respectively. Switching the woodrats between the distinctly different waters ensured that δ values of body water, hair, and tooth enamel could be modeled. Diet was not changed during these experiments. Depleted water samples were collected and analyzed monthly from the building where the animals were housed, and enriched water samples were analyzed periodically throughout the experiment. Water was switched on day 0 and blood and hair samples were collected from each control group on day 0. Hair samples were collected from the *N. cinerea* by plucking hair from the area at the base of the tail. After plucking, we shaved the area with a small electric shaver to ensure that all subsequent hair samples collected from the same area were produced after the water switch. Some length of hair below the skin

Table 1
Key to notation used in the text, models, tables, and figures

Term	Definition
δ_{bw}	δ value of body water
δ_{dw}	δ value of drinking water
$\delta^{18}O$	Isotope ratio for oxygen
δD	Isotope ratio for hydrogen
δ^t	Measured δ value at time t
δ^{eq}	Measured δ value at equilibrium
δ^{init}	Measured δ value prior to drinking water switch
F	Fraction of change at time t
δ_{tbw}	Estimated δ value of body water prior to evaporative enrichment
E_i	Estimate of the enrichment of body water due evaporative effects
δ_{mw}	Estimated δ value of metabolic water
δ_{fd}	δ value of food
$\delta^{18}O_{O_2}$	Estimated $\delta^{18}O$ value of O_2 absorbed in the lungs
$\delta^{18}O_{CO_2}$	Estimated $\delta^{18}O$ value of CO_2 produced during energy catabolization
p_{fd}	Estimated proportion of oxygen or hydrogen atoms from food
p_{mw}	Estimated proportion of oxygen or hydrogen atoms from metabolic water
p_{O_2}	Estimated proportion of oxygen atoms from atmospheric O_2
r	Molar quantity
$\delta^{18}O_{gw}$	Estimated O isotopic composition of gut water
δD_{fw}	Estimated H isotopic composition of follicle water
R_{bw}	Ratio of heavy to light isotope in body water
R_{dw}	Ratio of heavy to light isotope in drinking water
R_{fd}	Ratio of heavy to light isotope in food
R_{O_2}	Ratio of heavy to light isotope in O_2 absorbed in the lungs
R_{fw}	Ratio of heavy to light isotope in follicle water
R_{gw}	Ratio of heavy to light isotope in gut water
δ_h	δ value of hair
α_O	Fractionation between carbonyl oxygen and water
α_D	Fractionation between water and protein synthesis for hydrogen
$\alpha_{CO_2\text{-}bw}$	Fractionation between body water and CO_2
f_{init}	Initial mineral content of tooth enamel
δ_{mi}	δ value of the initial enamel at position i
δ_{ei}	δ value of fully mineralized enamel at position i
δ_{ci}	δ value of theoretical columns of enamel
δ_{di}	δ value of all columns included in each sample pit
l_a	Length of apposition of enamel matrix (mm)
l_m	Length of maturation of enamel matrix (mm)

(approximately 1 mm) remained and was part of the subsequent sample. We did not correct for this small amount of hair in our model. Hair samples were collected on days 0, 23, 31, 59, 71, 101, and 162 from various *N. cinerea*. We collected hair samples for 162 days to ensure that the δD and $\delta^{18}O$ of the hair was in isotopic equilibrium with the new drinking water. Blood samples were collected from 3 *N. cinerea* and 3 *N. stephensi* of the switched animals (group 1) on day 1 and the remaining animals from each species (group 2) were sampled on day 2. Woodrats were bled once per week to minimize stress on individual animals. Group 1 was also sampled on days 8, 16, 31, 71, and 101, and group 2 was sampled on days 10, 22, 64, and 101. Woodrats in the control group were sampled on days 14, 35, 64, and 101. We ended the experiment on day 32 for the *N. stephensi* because of prior experimental obligations. We collected approximately 200 μl of whole blood from the retro-orbital plexus of each woodrat.

Next, we switched the drinking water again for 3 of the *N. cinerea* 127 days after the first drinking water switch. Body water of woodrats is in equilibrium with drinking water after 30 days (127 days is ~10 half-lives). Two *N. cinerea* were switched from the enriched water to depleted water and 1 *N. cinerea* was switched from depleted water to the enriched water. We collected breath samples and analyzed both the C and O in CO_2 isotopically. Breath samples are non-invasive and allow repeated sampling of the same individual. We collected breath samples from each individual prior to the change in drinking water and 0.17, 0.5, 0.8, 1.2, 1.5, 1.8, 2.3, 3.2, 5.2, 7.2, 12.2, 15.2, 20.2, 26.2 days after the switch. All *N. cinerea* were sacrificed 27 days (day 162) after the second water switch and upper and lower incisors were extracted from each animal. We sacrificed the animals 27 days after the water switch to ensure that the tooth enamel of the incisors recorded the entire isotopic change from equilibrium with the starting water to equilibrium with the new water.

2.3. Sample analysis

The water in the blood samples was extracted cryogenically and all water samples were analyzed isotopically for O and H. Hair samples were also analyzed isotopically for O and H. Approximately 10–15% of the hydrogen in hair can exchange with water (liquid and vapor) and as a result, δD values must be corrected for exchangeable hydrogen (Bowen et al., 2005a). All reported δD of solid materials are for the non-exchangeable portion of hydrogen in these samples. Water samples were analyzed by injecting 0.5 μl of the sample onto a glassy carbon column heated to 1400 °C. The hair samples were analyzed by loading 150 μg into a silver capsule and pyrolosized at 1400 °C also in the presence of glassy carbon. The resultant H_2 and CO gases were separated chromatographically and introduced within a He stream into a ThermoFinnigan Delta Plus isotope ratio mass spectrometer. Samples were measured in duplicate and based on 1200 duplicate measurements of an internal standard; the average precision was 1.3‰ for δ^2H, and 0.17‰ for $\delta^{18}O$. The standard used for oxygen and hydrogen is Vienna Standard Mean Ocean Water [VSMOW].

Breath samples were collected by placing the woodrat in a metabolic chamber with the supply air scrubbed of CO_2 and water. An inline valve allowed us to ensure that no CO_2 was flowing into the chamber. The woodrat was in the chamber for 3–4 min, which allowed CO_2 levels to increase and stabilize. A 50 μl sample of breath was collected with a syringe and was immediately injected onto a gas chromatography column (Varian Poraplot Q©, 25 m length, 0.32 mm i.d.) attached to Finnigan MAT 252 mass spectrometer. The reported isotopic value for each animal is the mean of 4 injections. The variability of multiple breath samples over approximately 10 min was <0.3‰. Stable isotope ratios were calibrated to the PDB scale for C and O using a working standard calibrated to NBS-19. The same

reference standard was measured with ±0.3‰ over a several month period. Oxygen values are reported on the VSMOW scale using the conversion $\delta^{18}O_{VSMOW} = \delta^{18}O_{PDB} * 1.03086 + 30.86$.

$\delta^{18}O$ and $\delta^{13}C$ of mature enamel was analyzed using a CO_2 laser and by conventional H_3PO_4 methods. Laser ablation (Passey and Cerling, 2006) was used to measure the sequential change in the enamel for the three animals that were switched 27 days after the second water switch, and conventional H_3PO_4 analysis was used as a comparison between the laser and conventional methods. Values measured with H_3PO_4 were used to calculate ε^*_{AB} values. The outermost pigmented layer on the incisors was removed with a small electric hand grinder to ensure that we only analyzed enamel. Samples were loaded into the sample chamber and purged with helium overnight prior to analysis by laser ablation. Each individual measurement was the sum of 6 laser ablations at 25% power (~5–6 W), with a duration of 7.5 ms. CO_2 produced by the laser was cryogenically trapped and concentrated prior to injection into the GC (flow rate: 250 ml/min, GC temperature: 60 °C). Incisors were sequentially sampled starting at the distal end (oldest enamel) to the proximal end until significant charring was observed due to organic material in the immature enamel. We corrected the samples for CO_2 out-gassing from the teeth and fractionations associated with trapping and purging of the CO_2 by comparing with pre-chamber injected CO_2 standards. The same standards were used as above discussion of breath CO_2.

2.4. Modeling

2.4.1. Turnover of body water and hair

We used the reaction progress method to describe the turnover of O and H in the body water, breath CO_2, and hair (Cerling et al., 2007). Benefits to using the reaction progress variable include calculating the half-life for multiple-pool systems (Cerling et al., 2007). As well, results from an experiment in which animals are switched from one isotopically distinct source to a different source can be combined with the results from the reverse experiment, i.e, a reciprocal experimental design (Cerling et al., 2007). The reaction progress variable is a fractional method of modeling the turnover of an element within a tissue. The reaction progress variable is

$$\frac{\delta^t - \delta^{eq}}{\delta^{init} - \delta^{eq}} = e^{-\lambda t} \tag{4}$$

where δ^t is the measured δ value at time t, δ^{eq} is the δ value at equilibrium, and δ^{init} is the δ value prior to the drinking water switch ($t = 0$). The reaction progress variable scales the values between 0 and 1 and as a result, the preceding equation can be written as

$$\frac{\delta^t - \delta^{eq}}{\delta^{init} - \delta^{eq}} = (1 - F) \tag{5}$$

where F is the fraction of change that has occurred at time t. Eqs. (4) and (5) can be combined and written as

$$\ln(1 - F) = -\lambda t \tag{6}$$

which is a straight line, having the form:

$$y = mx + b \tag{7}$$

with a slope ($-\lambda$) and an intercept (b). The fractional contribution of each pool in a multiple-pool system is e^b for each pool. λ is a first order rate constant and the half-life of the element within the tissue is calculated according to the equation:

$$t_{1/2} = \ln(2)/\lambda \tag{8}$$

2.4.2. Body water modeling

We used a mass balance model to estimate the proportions of oxygen and hydrogen from drinking water, food, and molecular O_2 in the body water of the woodrats. This model differs from other body water models that estimate δ_{bw} in that, this model estimates the proportion (p) of oxygen and hydrogen atoms from all inputs based on measured and estimated δ values. This model also estimates the $\delta^{18}O$ of the CO_2 produced and of the metabolically generated water at the site of catabolization (metabolism resulting in the production of energy). The model incorporates the $\delta^{18}O$ and δD values of food, drinking water, molecular O_2, and the equilibrium fractionation ($\alpha = 1.0383$) between body water and CO_2 for the woodrats into the following series of equations to estimate the proportions of each major input. First, we estimated δD and $\delta^{18}O$ of body water prior to any enrichment effects (δ_{tbw}). δ_{tbw} is related to measured δ_{bw} by

$$\delta_{tbw} = \delta_{bw} - E_i \tag{9}$$

where E_i is an estimate of the enrichment of the body water due to evaporative effects. Next, the proportion of metabolic water in the larger body water pool was estimated with the following equation:

$$\delta_{tbw} = p * \delta_{mw} + (1 - p) * \delta_{dw} \tag{10}$$

where δ_{mw} is the estimated δ value of metabolic water, δ_{dw} is the measured δ value of drinking water and p is the proportion of metabolic water in the larger body water pool. In the case of hydrogen, the only source of hydrogen in metabolically generated water is food, thus:

$$\delta D_{mw} = \delta D_{fd} \tag{11}$$

In the case of oxygen, both food and atmospheric O_2 contribute oxygen atoms to metabolic water. During metabolic water formation CO_2 is produced; CO_2 is enriched relative to water, and as a consequence, it has a strong influence on $\delta^{18}O_{mw}$. Thus, the model incorporates the equilibrium fractionation between water and CO_2, and it includes the stoichiometry of the energy source catabolized. We assumed that carbohydrate was the energy source catabolized, and according to the stoichiometry of the following reaction:

$$C_6H_{12}O_6 + 6O_2 \rightarrow 6CO_2 + 6H_2O \tag{12}$$

carbohydrate is responsible for 33% and molecular O_2 is responsible for 67% of the oxygen that flows into metabolic water and CO_2. 67% of the oxygen input is incorporated into CO_2 and 33% is incorporated into water. $\delta^{18}O_{mw}$ is estimated by combining the stoichiometry of Eq. (12) with measured $\delta^{18}O$ values for food and atmospheric O_2 leading to:

$$0.33 * \delta^{18}O_{fd} + 0.67 * \delta^{18}O_{O_2} = 0.67 * \delta^{18}O_{CO_2} + 0.33 * \delta^{18}O_{mw} \quad (13)$$

where $\delta^{18}O_{fd}$ is the measured $\delta^{18}O$ value of the food, $\delta^{18}O_{O_2}$ is the $\delta^{18}O$ value for molecular oxygen absorbed in the lungs and $\delta^{18}O_{CO_2}$ is the $\delta^{18}O$ value of the CO_2. $\delta^{18}O_{mw}$ is estimated by combining the following equation for $\delta^{18}O_{CO_2}$ with Eq. (13).

$$\delta^{18}O_{CO_2} = \alpha * (1000 + \delta^{18}O_{mw}) - 1000 \quad (14)$$

The experimentally determined fractionation (α) between CO_2 and body water for the woodrats was 1.0383. We used a value of 15.1‰ for $\delta^{18}O_{O_2}$ that accounts for fractionation upon uptake in the lungs (Zanconato et al., 1992). Since both food and molecular O_2 contribute oxygen atoms to metabolic water, p_{mw} is multiplied by the stoichiometry of carbohydrate catabolization to estimate the proportion of each to metabolic water. The proportion of food oxygen in body water is related to p_{mw} by

$$p_{fd} = 0.33 * p_{mw} \quad (15)$$

and the proportion of molecular oxygen in body water is related to p_{mw} by

$$p_{O_2} = 0.67 * p_{mw} \quad (16)$$

We solved the equations simultaneously for each treatment group and we adjusted E_i to minimize the variation between estimates of p_{mw}, p_{fd}, and p_{O_2} for each treatment group.

We compared multiple published models that estimate $\delta^{18}O$ and δD of body water. All tested models are based on a model developed by Luz et al. (1984) for oxygen and modified by Schoeller et al. (1986a) for oxygen and hydrogen. We compared models developed by Bryant and Froelich (1995), Kohn (1996), and Gretebeck et al. (1997). We also used the equations developed by Kohn (1996) to estimate the molar influxes and effluxes of H_2O combined with measured and estimated values to estimate $\delta^{18}O$ and δD of body water for the woodrats. We used R notation to achieve better estimates of the enrichment of body water in deuterium and ^{18}O, and we used α values for the fractionation between body water and outputs (Schoeller et al., 1986a; Ritz et al., 1996; McKechnie et al., 2004). At steady state conditions, deuterium and ^{18}O of body water can be estimated for a one input and one output system using the following equation:

$$r_{in} * R_{in} = r_{out} * R_{out} * \alpha \quad (17)$$

where r is the molar quantity of the input or output, R is the ratio of the heavy isotope to the light isotope, and α is the fractionation between body water and the output. Eq. (17) can be extended for multiple inputs and outputs and subsequently solved for R_{bw}.

$$R_{bw} = \frac{\sum_{i=1}^{n} r_{in,i} * R_{in,i}}{\sum_{j=1}^{n} r_{out,j} * \alpha_{out,j}} \quad (18)$$

2.4.3. Hair model

We used a multiple-pool body water model that describes the flow of oxygen and hydrogen atoms into hair. We propose that the $\delta^{18}O_h$ is controlled by the isotopic composition of the gut water ($\delta^{18}O_{gw}$) and the δD_h is controlled by the isotopic composition of the intracellular water in the hair follicle (δD_{fw}). Oxygen atoms are primarily associated with C atoms in amino acids and the oxygen atoms exchange with water in the stomach (low pH) during digestion. Little exchange occurs after the amino acids enter the small intestine (neutral pH), and as a result, $\delta^{18}O_h$ is a function of $\delta^{18}O_{gw}$ which itself is a function of the $\delta^{18}O_{bw}$ and $\delta^{18}O$ of food ($\delta^{18}O_{fd}$). Thus, $\delta^{18}O_h$ will be related to $\delta^{18}O_{gw}$ by

$$\delta^{18}O_h = \alpha_o * (1000 + \delta^{18}O_{gw}) - 1000 \quad (19)$$

where α_o is the fractionation between carbonyl oxygen and water. We used an estimate of 1.0164 for α_o based on the measured carbonyl-oxygen fractionation between acetone and water for microbial cells (Kreuzer-Martin et al., 2003).

In the case of hydrogen, many of the hydrogen atoms in α-keratins can exchange with the intracellular water of the hair follicle during synthesis. The metabolic water generated inside the cell does not equilibrate instantaneously with and can be isotopically distinct from the extracellular water (Kreuzer-Martin et al., 2005, 2006) and as a result, the hydrogen atoms in the intracellular water will have a controlling influence on the isotopic composition of the hair. Hydrogen atoms in carboxyl, amide and sulfhydryl groups, but not C–H bonds, can exchange with intracellular water during protein synthesis. Thus, estimates for δD_h must include some estimate of both hydrogen atoms that can and cannot exchange with δD_{fw}. We assumed that C–H bonds on essential amino acids in α-keratins are related directly to dietary inputs and C–H bonds on non-essential amino acids are related to both recent dietary inputs and to the synthesis of amino acids by the animal. We used the amino acid composition of human hair as a proxy for woodrat hair, and 80% of the hydrogen in human hair is non-exchangeable, of which, 47% is associated with essential amino acids. Thus, we used a minimum estimate of 38% for the non-exchangeable hydrogen in keratin that is directly related to the diet. δD_h will be related to δD_{fw} by

$$\delta D_h = p_{fd} * \delta D_{fd} + (1 - p_{fd}) * (\alpha_D * (1000 + \delta D_{fw}) - 1000) \quad (20)$$

where α_D is the fractionation between water and protein synthesis for hydrogen and p_{fd} is the proportion of hydrogen from the food. We used an estimate of 1 for α_D. We assumed that 65% of the non-essential amino acids were synthesized by the woodrat, leading to the estimate that 52% of the hydrogen atoms in the hair were from the diet and the remainder was in isotopic equilibrium with δD_{fw}. We used a $\delta D_{fd} = -125$‰ for the food because proteins are generally more depleted than carbohydrates and the commercial diet was high in carbohydrates (Schoeller et al., 1986b).

We used a two-pool model to estimate $\delta^{18}O_{gw}$ and δD_{fw}. We first estimated δD_{bw} (Eq. (21)) and $\delta^{18}O_{bw}$ (Eq. (22)) using the proportions for the inputs and outputs of oxygen and hydrogen from Gretebeck et al. (1997):

$$R_{bw} = (R_{dw} * 0.81 + R_{fd} * 0.19)/(0.76 + 0.24 * 0.94) \quad (21)$$

$$R_{bw} = (R_{dw} * 0.62 + R_{O_2} * 0.24 * 0.992 + R_{fd} * 0.14)/(0.62 + 0.14 * 0.985 + 0.24 * 1.038) \quad (22)$$

where R_{bw} is the ratio of body water, R_{dw} is the ratio of drinking water, R_{fd} is the ratio of food, and R_{O_2} is the ratio of molecular oxygen. Next, we used the same equation but we substituted R_{bw} for R_{dw} to estimate δD_{fw} (Eq. (23)) and $\delta^{18}O_{gw}$ (Eq. (24)):

$$R_{fw} = (R_{bw} * 0.81 + R_{fd} * 0.19)/(0.76 + 0.24 * 1) \quad (23)$$

$$R_{fw} = (R_{bw} * 0.62 + R_{O_2} * 0.24 * 0.992 + R_{fd} * 0.14)/(0.62 + 0.14 * 1 + 0.24 * 1.038) \quad (24)$$

where R_{fw} is the ratio of the follicle water and R_{gw} is the ratio of the gut water. We assumed that there was no fractionated water loss within the follicle or the gut (i.e., $\alpha = 1$). After estimating R_{fw} (hydrogen) and R_{gw} (oxygen) we used Eqs. (19) and (20) to predict δ_h. We first used the proportions and α values from the Gretebeck et al. (1997) paper. Next, we modified the model by substituting the proportions for drinking water (O = 0.56; H = 0.70), food (O = 0.15; H = 0.30) and molecular O_2 (O = 0.30) estimated by our mass balance model (Table 2) for the proportions in the Gretebeck et al. (1997) model.

2.4.4. Tooth enamel modeling

We used forward modeling techniques to model the isotopic composition of the tooth enamel for the three *N. cinerea* that had their water switched during the second experiment. For complete description and examples of this technique, see Passey and Cerling (2002) and Passey et al. (2005a). Briefly, the forward modeling technique was developed for continually growing teeth because tooth enamel is not fully mineralized when it is first formed. The process of amelogenesis involves phases of prolonged mineral accumulation after initial deposition and, as a result, there is significant time-averaging of the isotopic signal in the enamel. Forward modeling requires measurements for the length of apposition (l_a) and length of maturation (l_m). Apposition is the area of the tooth where the enamel matrix is accreted and the maturation length is the length of tooth in which the remaining enamel matrix is completed. Forward modeling assumes that l_a, l_m, and the growth rate are constant. Maturation parameters were determined using micro computed tomography (micro-CT) imaging. We also assumed that the initial enamel deposition (f_{init}) had a mineral content of 25% (Passey and Cerling, 2002). The first step of the forward model is

$$\delta_{ei} = (f_{init} * \delta_{mi}) + (1 - f_{init}) * \frac{\sum_{n=i+1}^{i+l+l_m} \delta_{m_n}}{l_m} \quad (25)$$

where δ_{mi} is the initial isotopic composition and δ_{ei} is the isotope ratio of the fully mineralized enamel at position *i*. The remaining 75% mineralization reflects the average isotopic composition of the input signal. The appositional front is laid down at an angle, thus each sampling volume will theoretically include multiple layers of enamel accreted at different times. Thus, the second step of the forward model is

$$\delta_{ci} = \frac{1}{l_a} \sum_{n=i-l_a}^{i} \delta_{e_n} \quad (26)$$

where δ_{ci} is the isotope ratio of theoretical columns that transect and include multiple accreted layers. Finally, δ_{di} of each sample is calculated by averaging the isotopic signal from all columns included in each sampling pit:

$$\delta_{di} = \frac{1}{l_a} \sum_{n=i-\frac{1}{2}l_s}^{i-1+\frac{1}{2}l_s} \delta_{c_n} \quad (27)$$

3. RESULTS

3.1. Turnover of body water and hair

$\delta^{18}O_{bw}$ and δD_{bw} in *N. cinerea* and *N. stephensi* changed rapidly after a switch from depleted to enriched drinking water (Figs. 1 and 2). The half-life of ^{18}O in the body water was 3.6 days for the *N. cinerea* and 3.2 days for the *N. stephensi* (Fig. 1). The half-life of deuterium in the body water was 5.8 days for the *N. cinerea* and 3.8 days for the *N. stephensi* (Fig. 2). Drinking water was responsible for 56% of the oxygen atoms and 72% of the hydrogen atoms in the body water of the *N. cinerea* [(δ_{bw} depleted − δ_{bw} enriched)/(δ_{dw} depleted − δ_{dw} enriched)].

We collected breath samples from 3 *N. cinerea* and measured the change in $\delta^{18}O$ of body water by measuring $\delta^{18}O$ of breath CO_2 during the second water switch (Fig. 3). Fig. 3a shows the measured $\delta^{18}O$ values for all 3 animals. The reaction progress method allowed us to plot data collected from all animals on the same figure to determine any differences between treatment groups (Fig. 3b). Mean half-life of ^{18}O in breath CO_2 was 3.1 ± 0.1 days. We collected a breath sample and a blood sample from all 7 *N. cinerea* on day 162 prior to sacrifice, and $\delta^{18}O$ of breath CO_2 was in equilibrium with $\delta^{18}O$ of body water extracted from the blood samples ($\varepsilon^*_{breath\text{-}bw} = 38.3 \pm 0.3$). We can use the equation in Pflug et al. (1979) to estimate the body temperature of the *N. cinerea*. The estimated body temperature was 39.8 °C which is similar to the measured body temperature for other woodrats from the same genus (McLister et al., 2004).

δD of hair collected from the *N. cinerea* on day 0 was $-126 \pm 5‰$ and $\delta^{18}O$ of hair was $7.0 \pm 1.0‰$ (Fig. 4). After 162 days drinking the enriched water, δD of hair collected from the *N. cinerea* was $-10 \pm 6‰$ and $\delta^{18}O$ of hair was $20.9 \pm 0.5‰$ (Fig. 4). The turnover of the oxygen and hydrogen in the hair followed a multiple-pool model with the half-life of the short pool $\ll$23 days for oxygen and hydrogen. An accurate estimate for the half-life of the short pool was difficult to quantify because hair samples were not collected until 23 days after the change in the water. The half-life of the long pool was 144 days for oxygen and 51 days for hydrogen (Fig. 4). The short pool, for oxygen, was responsible for 83% of the oxygen atoms in the hair and the long pool was responsible for the remaining 17%. The short pool was responsible for 72% of the hydrogen atoms in the hair and the long pool was responsible for the remaining 28% (Fig. 4). Overall, drinking water sup-

Table 2
Mass balance model that estimates the proportion (p) of oxygen and hydrogen from drinking water, food, and atmospheric O_2 in the body water of the *N. cinerea*

Depleted drinking water					Enriched drinking water				
Measured values		Estimated values			Measured values		Estimated values		
	$\delta^{18}O$		$\delta^{18}O$	p		$\delta^{18}O$		$\delta^{18}O$	p
Oxygen									
$\delta^{18}O_{bw}$	−10.0	$\delta^{18}O_{tbw}$	−12.3		$\delta^{18}O_{bw}$	7.4	$\delta^{18}O_{tbw}$	5.1	
$\delta^{18}O_{O_2}$ [a]	15.1	$\delta^{18}O_{CO_2}$	30.6		$\delta^{18}O_{O_2}$ [a]	15.1	$\delta^{18}O_{CO_2}$	30.6	
$\delta^{18}O_{fd}$	24.0	$\delta^{18}O_{mw}$	−7.4		$\delta^{18}O_{fd}$	24.0	$\delta^{18}O_{mw}$	−7.4	
$\delta^{18}O_{dw}$	−16.1				$\delta^{18}O_{dw}$	15.0			
$\alpha_{CO_2\text{-}bw}$	1.0383				$\alpha_{CO_2\text{-}bw}$	1.0383			
		Metabolic water		0.44			Metabolic water		0.44
		Food		0.15			Food		0.15
		O_2		0.30			O_2		0.30
		Drinking water		0.56			Drinking water		0.56
E_o	2.3				E_o	2.3			
	δD		δD	p		δD		δD	p
Hydrogen									
δD_{bw}	−98	δD_{tbw}	−117		δD_{bw}	234	δD_{tbw}	207	
δD_{fd}	−109	δD_{mw}	−109		δD_{fd}	−109	δD_{mw}	−109	
δD_{dw}	−121				δD_{dw}	339			
		Food		0.30			Food		0.29
		Drinking water		0.70			Drinking water		0.71
E_D	22				E_D	22			

The model also estimates $\delta^{18}O$ of metabolic water generated in the cell by utilizing the equilibrium fractionation between water and CO_2. For each treatment group, the first column is measured values and the second column is the estimated δ values and proportions (see equations in Materials and methods).

[a] $\delta^{18}O_{O_2}$ is an estimate for the isotopic composition of the oxygen incorporated in the lungs.

plied 45% of the oxygen atoms and 25% of the hydrogen atoms in the hair of the *N. cinerea* [(δ_h depleted − δ_h enriched)/(δ_{dw} depleted − δ_{dw} enriched)].

3.2. Body water modeling

We developed a mass balance model that uses measured δ_{bw} values to estimate the proportions of food, molecular O_2, and drinking water in the body water of the *N. cinerea* (Table 2). The proportions estimated for each treatment group were similar when an enrichment factor (E_o) of 2.3‰ was subtracted from measured $\delta^{18}O_{bw}$. The model estimated that food, molecular O_2 and drinking water were responsible for 15%, 30%, and 56% of the oxygen in body water, respectively. The model also produced an estimate of −7.4‰ for $\delta^{18}O_{mw}$ (Table 2). In the case of hydrogen, the proportions estimated for each treatment group were similar when an enrichment factor (E_D) of 22‰ was subtracted from measured δD_{bw}. The model estimated that food and drinking water were responsible for 29% and 71% of the hydrogen in body water, respectively (Table 2).

We compared measured δ_{bw} values with estimated δ_{bw} values from multiple published models (Table 3). We also modified specific models to more closely reflect diet composition and the total energy expenditure (TEE) and total water flux (TWF) of the *N. cinerea* (Table 3). Table 4 supplies the various parameters and values used in the body water models. Overall, the linear regression compiled by Bryant and Froelich (1995) with data from three studies on lab rats and the Gretebeck et al. (1997) model most accurately estimated δ_{bw} of the *N. cinerea* (Table 3). After modification, the influx/efflux model based on the Kohn (1996) model and the Gretebeck et al. (1997) model reliably estimated $\delta^{18}O_{bw}$ and δD_{bw} (Table 3).

3.3. Hair model

We used a multiple-pool body water model to describe the flow of oxygen and hydrogen atoms into the hair of the *N. cinerea* (Table 5). We first used the proportions for the inputs and outputs of oxygen and hydrogen described in Gretebeck et al. (1997) body water model for humans. This model estimated $\delta^{18}O_{bw}$ and $\delta^{18}O_h$ for both treatment groups within 1.5‰ of measured values (Table 5). Next, we modified the input and output proportions to match the proportions estimated by the mass balance model (Table 2). The accuracy of the estimates of $\delta^{18}O_{bw}$ for both treatment groups increased (<0.2‰ from measured values), but this modification decreased the accuracy of the estimate for $\delta^{18}O_h$ of the enriched group (Table 5). In the case of hydrogen, the Gretebeck et al. (1997) model reliably estimated δD_{bw} and δD_h for the depleted treatment group, but poorly estimated both δD_{bw} and δD_h for the enriched group (Table 5). Using the proportions of drinking water and food estimated from the mass balance model did not significantly change the estimate for δD_{bw} and δD_h for the depleted group but did significantly increase the accuracy of the estimate for the enriched group (Table 5).

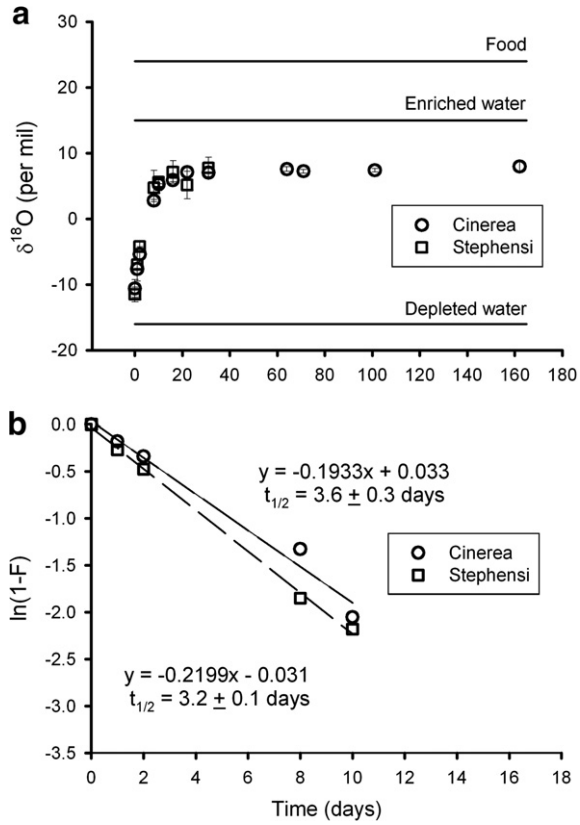

Fig. 1. $\delta^{18}O$ of the body water collected from *N. cinerea* (circles) and *N. stephensi* (squares) after a change in drinking water. Animals were switched from the depleted water to the enriched water. (b) Reaction progress variable ($\ln(1-F)$) calculated from data of (a).

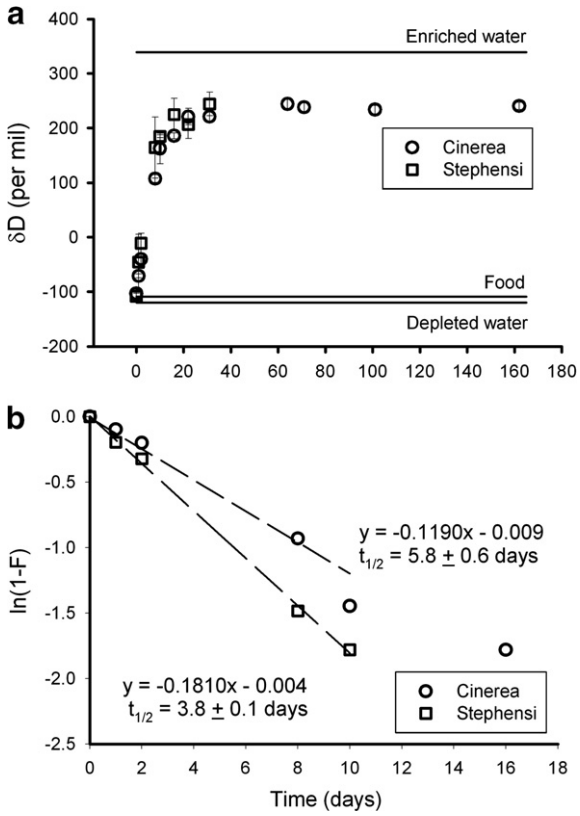

Fig. 2. δD of the body water collected from *N. cinerea* (circles) and *N. stephensi* (squares) after a change in drinking water. Animals were switched from the depleted water to the enriched water. (b) Reaction progress variable ($\ln(1-F)$) calculated from data of (a).

3.4. Tooth enamel modeling

Tooth enamel recorded the change in drinking water for the three *N. cinerea* and the forward model provided relatively accurate predictions for $\delta^{18}O$ of the enamel based on the change in $\delta^{18}O$ of the body water input signal (Fig. 5). Incisors collected from the animals that had been maintained on either the depleted water or the enriched water revealed that body water and tooth enamel were in isotopic equilibrium with $\varepsilon^*_{\text{enamel-bw}} = 27.0 \pm 2.1$ and $\varepsilon^*_{\text{enamel-breath}} = -10.7 \pm 1.9‰$ (Table 6).

$\delta^{13}C$ of breath CO_2 and $\delta^{13}C$ of the enamel were uniform for all seven animals with $\varepsilon^*_{\text{breath-diet}}$ equal to -0.8 ± 0.5 (Table 7). $\delta^{13}C$ of tooth enamel measured by laser ablation was slightly more variable than $\delta^{13}C$ of tooth enamel measured using the H_3PO_4 method, but overall, both methods were reliable and $\varepsilon^*_{\text{laser-}H_3PO_4}$ was $-1.9 \pm 0.4‰$ (Table 7). Using the H_3PO_4 method, $\varepsilon^*_{\text{enamel-breath}}$ was $11.8 \pm 0.5‰$ and $\varepsilon^*_{\text{enamel-diet}}$ was $11.0 \pm 0.1‰$.

4. DISCUSSION

4.1. Turnover and modeling of body water

It is clear that drinking water influences the isotope composition of body water, hair, and tooth enamel of small mammals. We manipulated the isotope composition of drinking water supplied to woodrats to resolve the relationships between drinking water and tissue. We also quantified the turnover of the body water within the woodrats and the subsequent turnover of the oxygen and hydrogen within the hair and tooth enamel. The turnover of the oxygen and hydrogen in the body water of the woodrats followed a one-pool model and the half-life of the oxygen and hydrogen in the body water was between 3 and 6 days. We measured the change in the δ_{bw} by extracting water from blood samples and by collecting breath CO_2 samples. CO_2 and body water were in equilibrium and breath samples were a non-invasive technique that allowed us to repeatedly measure the same animal.

The turnover of the body water in the woodrats was at the higher end of the range observed for laboratory rats (1.4–3.3 days) which are similar in size to the *N. cinerea* and *N. stephensi* (Thompson, 1953; Longinelli and Padalino, 1980; Luz et al., 1984). However, the woodrats inhabit relatively arid environments and may have been adapted to low-water environments. Nevertheless, two weeks after a water switch the body water of the woodrats had nearly reached isotopic equilibrium. As a consequence, body water samples collected from small mammals two weeks after a change in location or resource use will represent the new drinking water.

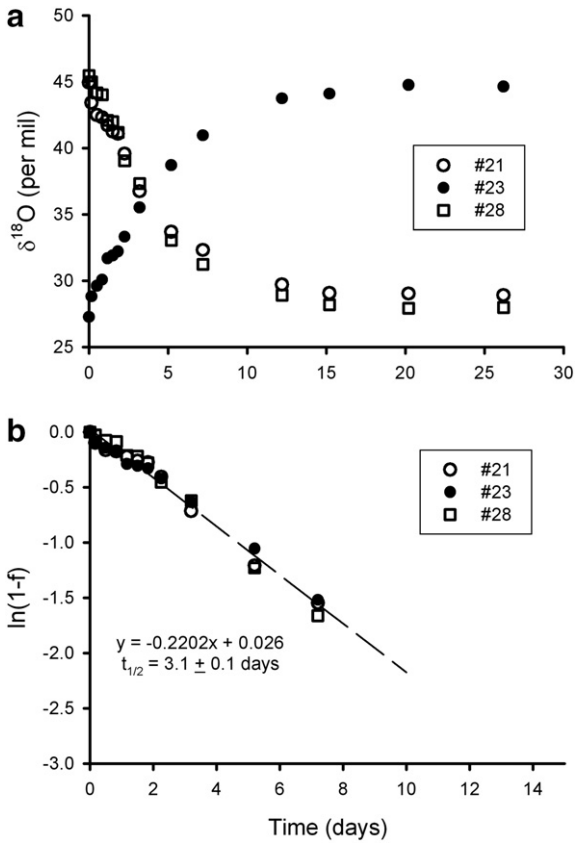

Fig. 3. $\delta^{18}O$ of the breath collected from 3 *N. cinerea* after a change in drinking water. Two animals were switched from the enriched water to the depleted water and 1 animal was switched from the depleted water to the enriched water. (b) Reaction progress variable ($\ln(1 - F)$) calculated from data of (a).

Overall, drinking water was responsible for 71% of the hydrogen and 56% of the oxygen in the body water of the *N. cinerea*. Food was responsible for the remaining 29% of the hydrogen. Food and molecular O_2 both supply oxygen to the body water pool and a mass balance model estimated that food and molecular O_2 were responsible for 15% and 30% of the oxygen in the body water, respectively (Table 2).

Similar estimates for the contribution of food oxygen and molecular O_2 could have been made by multiplying the proportion of body water that is not from drinking water (44%) by 67% and 33% (from the stoichiometry of carbohydrate catabolization). However, the mass balance model includes a theoretical estimate for $\delta^{18}O$ of the metabolic water generated within the cell by incorporating the equilibrium fractionation between body water and CO_2, thus displaying the strong influence of CO_2 in determining $\delta^{18}O_{bw}$. We assumed that only carbohydrate was utilized as an energy source and that the measured δ values for the bulk food were representative of the δ values of the carbohydrate catabolized in the cell. The diet was a high-carbohydrate diet with 14% protein and less than 3% fat. Therefore, the woodrats most likely routed carbohydrate directly to the cells to be used as energy and the δ value measured was similar to the δ value of the carbohydrate. We also assumed that $\delta^{18}O$ of the molecular O_2 utilized in the cell was 15.1‰. This assumption was based on experimentally derived values and is commonly used in other body water models (Zanconato et al., 1992; Kohn, 1996; Gretebeck et al., 1997).

We compared measured δ_{bw} for the *N. cinerea* with estimated δ_{bw} values from multiple published models (Table 3). The first model, from Table 1 in Bryant and Froelich (1995), is the compilation of three studies on the turnover of oxygen in the body water of lab rats (see Longinelli and Padalino, 1980; Luz et al., 1984; Luz and Kolodny, 1985). Overall, the relationship between $\delta^{18}O_{bw}$ and $\delta^{18}O_{dw}$ ($\delta^{18}O_{bw} = 0.56 * \delta^{18}O_{dw} - 0.33$) for the lab rats estimated $\delta^{18}O_{bw}$ of the woodrats within 1‰ of measured values for both treatment groups (Table 3). Both the regression and our mass balance model estimated that 56% of the oxygen in the body water of the lab rats and the woodrats was from drinking water. The lab rats and the woodrats are similar in size and commercial rat food and the commercial rabbit food (fed to the woodrats) were likely similar in water content and macronutrient composition. Although, the proportion of body water that was related to drinking water was the same for the lab rats and the woodrats, there were differences in turnover, perhaps reflecting physiological adaptations to arid environments for the woodrats.

The Bryant and Froelich (1995) model was designed for herbivores >1 kg, yet, it estimated $\delta^{18}O_{bw}$ for the enriched animals within 1‰ of measured values (Table 2). However, the Bryant and Froelich (1995) model poorly estimated $\delta^{18}O_{bw}$ for the depleted animals and when the measured $\delta^{18}O$ of food was used instead of the estimated value; the estimates were unreliable for both treatment groups. We modified the input parameters of the Bryant model to more closely match the measured and estimated values for total water flux (TWF) and total energy expenditure (TEE), but the accuracy was not increased. The Bryant model predicts that $\delta^{18}O_{bw}$ of smaller animals should be more enriched relative to $\delta^{18}O_{dw}$ than larger mammals. However, this effect was overestimated for the woodrats.

Kohn (1996) improved on earlier body water models by including diet composition and physiological adaptations in his model of δ_{bw}. Briefly, the Kohn model predicts $\delta^{18}O_{bw}$ by estimating the molar fluxes for all sources of oxygen including drinking water, molecular O_2, food oxygen, food water, water vapor gain, transcutaneous water loss, water lost due to breathing, expelled CO_2, and urine combined with the influence of temperature, relative humidity and physiological adaptations such as the method used by an animal to dissipate excess body heat. Overall, the Kohn model estimated $\delta^{18}O_{bw}$ within 1‰ for the depleted group, but modeled $\delta^{18}O_{bw}$ was more enriched than measured for the enriched group (Table 3). We substituted the measured food values for estimated values, and the accuracy was not improved. We used the fluxes estimated by the equations in the Kohn (1996) model to estimate the daily fluxes of hydrogen and we added the measured and estimated values for TEE, diet composition and the amount of drinking water consumed by the woodrats to create a model specific to the woodrats (Tables 3 and 4). This model accurately

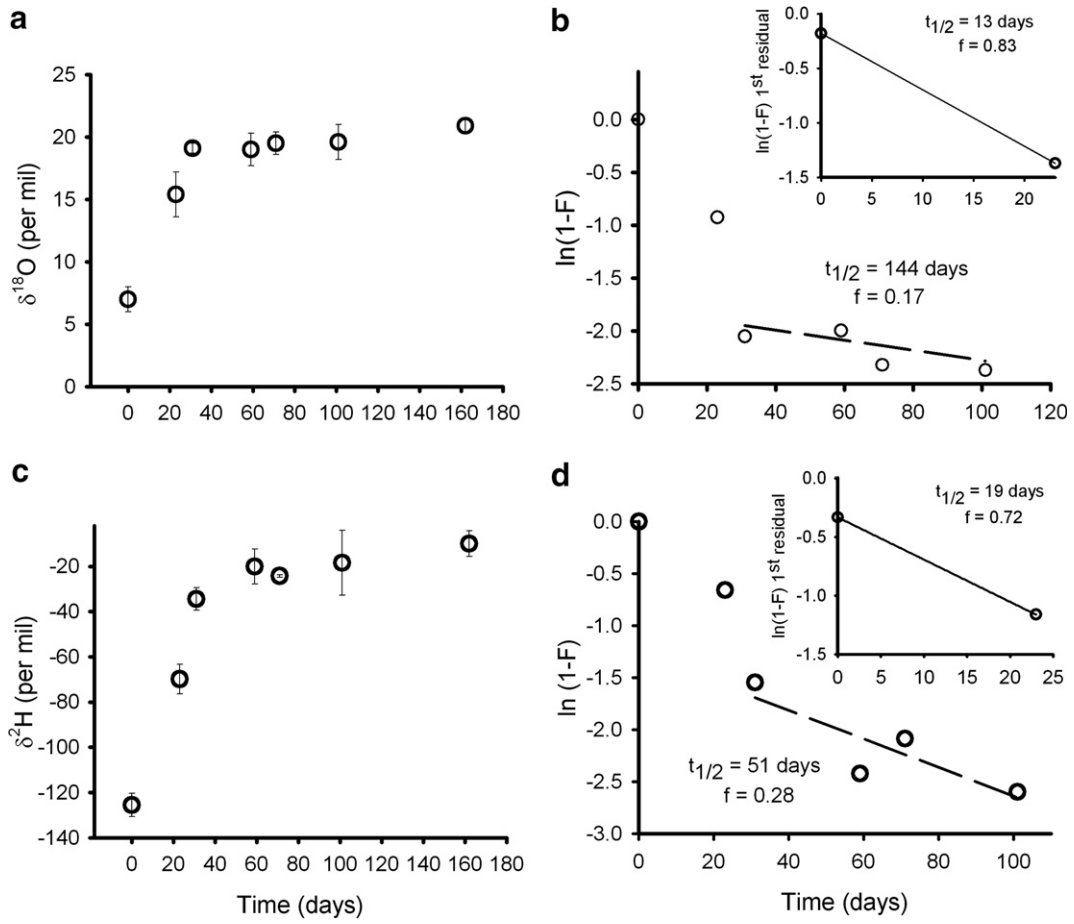

Fig. 4. $\delta^{18}O$ (a) and δD (c) of the hair collected from *N. cinerea* after a change in drinking water. Animals were switched from the depleted water to the enriched water. (b) and (d) Reaction progress variable ($\ln(1 - F)$) calculated from data of (a) and (c).

Table 3
Comparison between measured δ_{bw} values and modeled δ_{bw} values from multiple published body water models

Treatment	δ_{bw}							
	Measured	Rats[a]	Bryant[b]	Bryant[c] modified	Kohn[d]	Kohn[e] influx/efflux	Gretebeck[f]	Gretebeck[g] modified
Oxygen								
Depleted	-10.0 ± 0.6	−9.3	−1.8	−5.3	−9.6	−7.9	−10.9	−10.2
Enriched	7.4 ± 0.3	8.1	7.9	10.6	11.0	7.2	8.3	7.4
Hydrogen								
Depleted	-98 ± 4					−93	−106	−103
Enriched	234 ± 10					248	272	234

[a] $\delta^{18}O_{bw} = 0.56 * \delta^{18}O_{dw} - 0.33$; From Table 1 in Bryant and Froelich (1995); Bryant and Froelich combined data from three studies (Longinelli and Padalino, 1980; Luz et al., 1984; Luz and Kolodny, 1985) on the turnover of oxygen in the body water of lab rats to produce this relationship.
[b] $\delta^{18}O_{bw}$ calculated using model equations and $\delta^{18}O$ values developed by Bryant and Froelich (1995).
[c] $\delta^{18}O_{bw}$ calculated using model and $\delta^{18}O$ values developed by Bryant and Froelich (1995) combined with measured and estimated values for water influxes and effluxes; see Table 3.
[d] $\delta^{18}O_{bw}$ calculated using model and $\delta^{18}O$ values developed by Kohn (1996).
[e] $\delta^{18}O_{bw}$ and δD_{bw} calculated using influx and efflux equations developed by Kohn (1996) for oxygen and extrapolated for hydrogen.
[f] $\delta^{18}O_{bw}$ and δD_{bw} calculated using model developed by Gretebeck et al. (1997).
[g] $\delta^{18}O_{bw}$ and δD_{bw} calculated using model developed by Gretebeck et al. (1997) but modified to more closely resemble the woodrats.

estimated $\delta^{18}O_{bw}$ for the enriched group and was within 2‰ for the depleted animals; it also adequately estimated δD_{bw} for both groups. Body water models can be accurate when detailed physiological is available for each individual species. However, this model is complex and may be difficult to use when detailed information is not available.

Table 4
Parameters, measured and estimated quantities, δ and α values and the source for each used in the body water models

Parameter/variable	Value	δ	α	Source
Mb (g)	300			
Temperature (°C)	25			
RH	30			
TEE (kJ)	225[a]			Estimated from kJ of food consumed
Drinking water (moles)	1.3			DW(g) = 0.05(Mb) + 8.3 (measured)
Water economy index	0.16[b]			Adjusted to approximate DW above
Pant/sweat ratio	1			Kohn (1996)
% Water in feces	50			Estimated
Food (g)	20			Teklad – 2031 High Fiber Rabbit Diet
Carb (g)	8.6			Total food = 0.067/g Mb (measured)[c]
Lipid (g)	0.5			Carb, lipid, protein, fiber, ash, and water estimated from Teklad
Protein (g)	2.9			diet composition information
Fiber and ash (%)	30			
Food water (%)	10			
$\delta^{18}O_{O_2}$		15.1		Zanconato et al. (1992)
$\delta^{18}O$ depleted water		-16.1 ± 0.2		Measured
$\delta^{18}O$ enriched water		15.0 ± 0.2		Measured
$\delta^{18}O$ food		24.0 ± 0.2		Measured
δD depleted water		-121 ± 1		Measured
δD enriched water		339 ± 2		Measured
δD food		-109 ± 4		Measured
Oxygen				
$\alpha_{water\text{-}vapor}$			1.009	Water vapor gain (Horita and Wesolowski, 1994)
$\alpha_{trans\text{-}bw}$			0.981	Transcutaneous water loss (Schoeller et al., 1986a)
$\alpha_{oral\text{-}bw}$			0.991	Oral water loss (Schoeller et al., 1986a)
$\alpha_{nasal\text{-}bw}$			0.991	Nasal water loss (Kohn, 1996)
$\alpha_{CO_2\text{-}bw}$			1.038	Measured
$\alpha_{vapor\text{-}bw}$			0.992	Gretebeck et al. (1997)—used in Gretebeck model
Hydrogen				
$\alpha_{water\text{-}vapor}$			1.079	Water vapor gain (Horita and Wesolowski, 1994)
$\alpha_{trans\text{-}bw}$			0.935	Transcutaneous water loss (Schoeller et al., 1986a)
$\alpha_{oral\text{-}bw}$			0.946	Oral water loss (Schoeller et al., 1986a)
$\alpha_{nasal\text{-}bw}$			0.957	Estimated from $\alpha_{nasal\text{-}bw}$ above; Evap. slope = 5
$\alpha_{vapor\text{-}bw}$			0.94	Gretebeck et al. (1997)—used in Gretebeck model

[a] TEE was greater than estimated for desert rodents but less than estimated for all rodents (Nagy et al., 1999).
[b] WEI of 0.16 resulted in the same moles of drinking water as measured.
[c] Measured for *N. cinerea*.

The model developed by Gretebeck et al. (1997) for humans minimizes the inputs and outputs of oxygen and hydrogen, and does not include physiological or climatic variables, yet, it estimated $\delta^{18}O_{bw}$ within 1‰ for both groups and it reliably estimated δD_{bw} for the depleted group (Table 3). When the proportions of food, drinking water and molecular O_2 were modified to match the estimated proportions from the mass balance model (Table 2), the Gretebeck model reliably estimated $\delta^{18}O_{bw}$ and δD_{bw} for both groups (Table 3). The Gretebeck model, as well as the other models, is based on linear relationships between δ_{dw} and δ_{bw}. As a result, slight variations in the relative proportion of each input (drinking water, food, atmospheric O_2) will strongly influence predicted δ_{bw} values, especially for a system in which the δ values of the drinking water differ by 30‰ and 460‰ for oxygen and hydrogen, respectively. Our experimental system was designed to ensure that differences between the treatment groups were large enough that modeling efforts of δ values of body water, hair, and tooth enamel were successful.

4.2. Turnover of hair

Our data demonstrate that oxygen and hydrogen in drinking water is incorporated into hair keratin. Drinking water was responsible for 45% of the oxygen and 25% of the hydrogen in the hair of the woodrats. This is similar to estimates for the contribution of hydrogen to proteinaceous tissues in birds and to hair in humans (Hobson et al., 1999; Sharp et al., 2003). The turnover of the oxygen and hydrogen within the hair followed a multiple-pool model, similar to that observed in the turnover of carbon in the hair of horses (Ayliffe et al., 2004). Diet was static in this experiment and drinking water was the only parameter modified. Thus, the short pool was related to drinking water and the long pool was related to the turnover of other tissues within the woodrat. Our estimates for the half-lives and the relative proportion of each pool to final tissue signature may be inaccurate because rodents grow hair in waves across the body. We did stimulate the woodrats to replace the plucked and shaved hair. However, there was some uncertainty in estimating the start of hair growth

Table 5
Comparison between measured δ_{bw} and δ_h values and modeled δ_{bw} and δ_h values for the *N. cinerea*

Treatment	Gretebeck et al. (1997) model and parameters				Updated model and parameters				Measured	
	δ_{bw}	$\delta_{fw/gw}$	ε	δ_h	δ_{bw}	$\delta_{fw/gw}$	ε	δ_h	δ_{bw}	δ_h
Oxygen										
Depleted	−10.9	−8.7	16.4	7.5	−10.2	−8.9	16.4	7.3	−10.0 ± 0.6	7.0 ± 1.0
Enriched	8.3	3.0	16.4	19.5	7.4	1.0	16.4	17.4	7.4 ± 0.3	20.9 ± 0.5
Hydrogen										
Depleted	−110	−114	0	−122	−111	−116	0	−123	−98 ± 4	−126 ± 5
Enriched	268	193	0	23	225	126	0	−8	234 ± 10	−10 ± 6

prior to each collection which may have affected our estimates of pool size and half-life. Nevertheless, the data suggest that there are multiple pools of oxygen and hydrogen that can flow into hair.

We tested a model that estimates the δD_h and $\delta^{18}O_h$ based on the predicted δD of the water within the hair follicle and the $\delta^{18}O$ of the gut water. We developed a two pool model for predicting the isotopic composition of the hair because the relationship between δ_{bw} and δ_h for the two treatment groups was not accurate unless the multiple-pool model was used.

We used the Gretebeck body water model to estimate δD_{bw} and $\delta^{18}O_{bw}$ and second to estimate δD_{fw} and $\delta^{18}O_{gw}$. Next, we estimated the relative contribution of oxygen and hydrogen from the intracellular water and from the diet that was used in hair synthesis. We assumed that all oxygen in hair was in isotopic equilibrium with the gut water and a portion of the hydrogen was in equilibrium with the follicle water. The remaining source of hydrogen in the hair was related to the diet by the amount of essential amino acids in hair keratin and to an estimate of the amount of routing of non-essential amino acids directly from the diet into hair synthesis.

The model robustly estimated $\delta^{18}O_h$ for both treatment groups and δD_h for the depleted group, but poorly estimated δD_h for the enriched group (Table 5). This discrepancy was related to the poor estimate that the original Gretebeck model produced for δD_{bw} for the enriched group (Table 5). When the input proportions of drinking water, food, and molecular O_2 were changed to those estimated by the mass balance model, the estimates of δD_{bw} and δD_h for both groups were accurate and the estimates of $\delta^{18}O_{bw}$ and $\delta^{18}O_h$ were also accurate. Thus, δD_h values were sensitive to the relative proportions of food and drinking water used in the model. δD_h values were also moderately sensitive to the estimated proportion of routing of non-essential amino acids directly from the diet into hair synthesis. As long as the estimates of routing ranged between 30% and 50%, estimated δD_h values were within 10‰ of measured values. The commercial diet fed to the woodrats was nutritionally-adequate and thus, we might expect that the animal would route 100% of the amino acids directly from the diet into protein synthesis and not expend energy synthesizing a portion of the non-essential amino acids. However, animals fed nutritionally-adequate diets do route carbon skeletons from non-dietary protein sources into protein synthesis (Podlesak and McWilliams, 2006). As a consequence, an estimate of 50% direct routing from the diet and 50% synthesis of the non-essential amino acids in the keratin of the woodrats does not appear out of line.

The hair model was relatively insensitive to variation in the δ values of food. Estimated $\delta^{18}O_h$ values varied <2‰ from measured values when $\delta^{18}O_{fd}$ values between 20‰ and 30‰ were used, and estimated δD_h values varied <15‰ from measured values when δD_{fd} values between −115‰ and −150‰ were used. Overall, the hair model reliably estimated the oxygen and hydrogen isotopic composition of the woodrat hair.

4.3. Tooth enamel

Tooth enamel is routinely used to reconstruct the diet of animals and to also reconstruct past climate (Fricke and O'Neil, 1996; Hoppe et al., 2004). In general, enamel from large mammals is used because most analysis methods require more enamel than can be safely extracted from the teeth of small mammals (Passey and Cerling, 2006). Recently, Passey and Cerling (2006) developed a method using laser ablation to measure the $\delta^{18}O$ of tooth enamel in very small teeth. We used this method to track the change in drinking water for the *N. cinerea* by measuring the $\delta^{18}O$ of bulk enamel sequentially along the length of the continually growing incisors (Fig. 5).

We sequentially sampled the upper and lower incisors of 3 *N. cinerea*, 2 that were switched from the enriched drinking water to the depleted drinking water and a third that was switched from the depleted drinking water to the enriched water. Each incisor was sampled from the distal end, the oldest section of enamel, to the proximal end. The 3 animals had been switched to new drinking water 27 days prior to sacrifice and in general, all incisors recorded the change in $\delta^{18}O$ of enamel from isotopic equilibrium with the initial drinking water to isotopic equilibrium with the new drinking water (Fig. 5). The lower incisor extracted from animal #23 did not record the initial drinking water because the growth rate was much faster than the growth rates for the other incisors. Growth rates for the other incisors ranged from 0.6 to 0.9 mm day^{-1}, whereas the growth rate of the lower incisor from #23 was 1.6 mm day^{-1}. This lower incisor was damaged and its higher growth rate was likely due to the animal attempting to repair the tooth and reestablish the correct alignment between its upper and lower incisors. Overall, these data indicate that laser ablation analysis of continually-growing incisors can be used to identify recent changes in drinking water due to a change in resource use or due to a change in location.

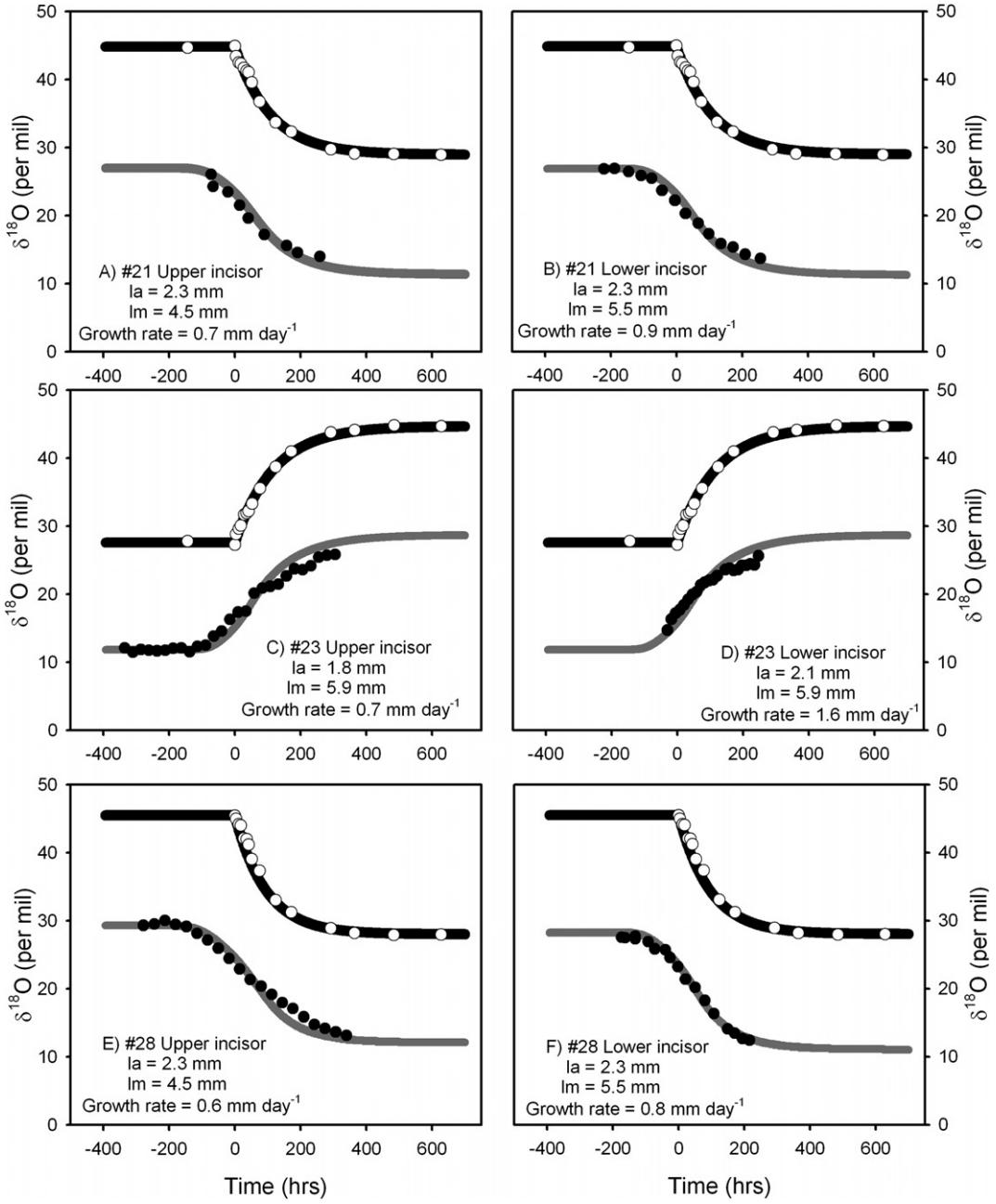

Fig. 5. $\delta^{18}O$ of the modeled body water (black line), of the measured body water (open circles), modeled tooth enamel (gray line) and measured enamel (black circles) for the upper and lower incisors from the 3 *N. cinerea* that had their water switched 27 days prior to the end of the experiment.

These data can also be used to evaluate the forward modeling techniques developed by Passey and Cerling (2002) to estimate $\delta^{18}O$ of tooth enamel based on $\delta^{18}O$ of the input signal. The input signal is the body water, and if the change in $\delta^{18}O_{bw}$ is known or can be estimated, forward modeling can be used to predict the change in the $\delta^{18}O$ values of enamel in continually-growing teeth. Approximately 75% of enamel mineralization occurs after initial deposition and changes in the input signal will influence the isotopic composition of tooth enamel throughout mineralization. As a result, distinct changes in $\delta^{18}O_{bw}$ will influence the isotopic composition of tooth enamel deposited prior to and after the change in drinking water. The forward model, by incorporating the growth rate, appositional length and maturation length, corrects for the time-averaging of the $\delta^{18}O$ of tooth enamel due to this extended mineralization.

Overall, the forward model closely predicted the measured tooth enamel signal, although there are small but important differences. In particular, the predicted (forward model) rate of isotope change is higher than the measured rate of change in many of the teeth (most pronounced in

Table 6
Measured $\delta^{18}O_{dw}$, $\delta^{18}O_{bw}$, $\delta^{18}O_{breath}$, $\delta^{18}O_{enamel}$ values and isotope spacing between body water, breath, and enamel for the *N. cinerea*

Animal	Exp. 1	Exp. 2	$\delta^{18}O_{bw}$	$\delta^{18}O_{breath}$	Laser	H_3PO_4	$\varepsilon^*_{laser\text{-}H_3PO_4}$	$\varepsilon^*_{breath\text{-}bw}$	H_3PO_4	
	$\delta^{18}O_{dw}$	$\delta^{18}O_{dw}$			$\delta^{18}O_{enamel}$	$\delta^{18}O_{enamel}$			$\varepsilon^*_{enamel\text{-}breath}$	$\varepsilon^*_{enamel\text{-}bw}$
3	15.0	15.0	8.6	47.4 ± 0.5	*	36.2	NA	38.4 ± 0.5	-10.7 ± 0.5	27.3
21	15.0	−16.1	−8.9	28.9	**	NA	NA	38.1	NA	NA
23	−16.1	15.0	5.6	44.6	**	NA	NA	38.8	NA	NA
25	−16.1	−16.1	−9.2	28.7 ± 0.3	12.0 ± 0.5	19.9	-7.8 ± 0.5	38.2 ± 0.3	-8.5 ± 0.3	29.4
28	15.0	−16.1	−10.3	28.0	**	NA	NA	38.7	NA	NA
29	15.0	15.0	7.1	45.5 ± 0.1	26.4 ± 0.4	NA	NA	38.1 ± 0.1	NA	NA
30	15.0	15.0	8.2	46.5 ± 0.1	28.9 ± 1.3	32.8	-3.8 ± 1.3	38.0 ± 0.1	-13.1 ± 0.1	24.4
						Averages:	-5.8 ± 2.0	38.3 ± 0.3	-10.7 ± 1.9	27.0 ± 2.1

$\delta^{18}O_{enamel}$ was measured using laser ablation and conventional H_3PO_4 methods.
Note: ±values are 1σ for δ values and propagated error for ε values.
* All enamel was consumed in the H_3PO_4 method.
** Enamel from animals 21, 23, and 28 were sequentially sampled.

Table 7
Measured $\delta^{13}C_{diet}$, $\delta^{13}C_{breath}$, and $\delta^{13}C_{enamel}$ values and isotope spacing between body water, breath, and enamel for the *N. cinerea*

Animal	$\delta^{13}C_{diet}$	$\delta^{13}C_{breath}$	Laser	H_3PO_4	$\varepsilon^*_{laser\text{-}H_3PO_4}$	$\varepsilon^*_{breath\text{-}diet}$	H_3PO_4	
			$\delta^{13}C_{enamel}$	$\delta^{13}C_{enamel}$			$\varepsilon^*_{enamel\text{-}breath}$	$\varepsilon^*_{enamel\text{-}diet}$
3	-25.9 ± 0.4	-26.4 ± 0.2	*	-15.2 ± 0.2	NA	-0.5 ± 0.5	11.5 ± 0.3	11.0 ± 0.4
21	-25.9 ± 0.4	-26.1 ± 1.1	-16.9 ± 0.2	-15.2 ± 0.2**	-1.7 ± 0.3	-0.2 ± 1.2	11.2 ± 1.1	11.0 ± 0.4
23	-25.9 ± 0.4	-26.7 ± 0.5	-17.0 ± 0.9	−15.4	-1.6 ± 0.9	-0.8 ± 0.6	11.6 ± 0.5	10.8 ± 0.4
25	-25.9 ± 0.4	-26.5 ± 0.6	-16.3 ± 0.3	−15.1	-1.3 ± 0.3	-0.6 ± 0.7	11.7 ± 0.6	11.1 ± 0.4
28	-25.9 ± 0.4	-27.1 ± 0.4	-17.6 ± 0.9	-15.2 ± 0.2	-2.4 ± 1.0	-1.2 ± 0.6	12.2 ± 0.4	11.0 ± 0.4
29	-25.9 ± 0.4	-27.5 ± 0.3	-17.2 ± 0.3	-15.2 ± 0.2**	-2.1 ± 0.3	-1.7 ± 0.5	12.7 ± 0.3	11.0 ± 0.4
30	-25.9 ± 0.4	-26.5 ± 0.1	-17.3 ± 0.5	-15.2 ± 0.1	-2.1 ± 0.5	-0.6 ± 0.4	11.6 ± 0.2	11.0 ± 0.4
	Averages:	-26.7 ± 0.5	-17.0 ± 0.4	-15.2 ± 0.1	-1.9 ± 0.4	-0.8 ± 0.5	11.8 ± 0.5	11.0 ± 0.1

$\delta^{13}C_{enamel}$ was measured using laser ablation and conventional H_3PO_4 methods.
Note: ±values are 1σ for δ values and propagated error for ε values.
* All enamel was consumed in the H_3PO_4 method.
** Average value because these teeth were used specifically for laser ablation.

Fig. 5c and e). This may indicate a mismatch between the assumed pattern of mineral uptake (linear with respect to time and distance) versus the actual pattern. Indeed, the microCT images of the developing teeth show that the pattern of mineral uptake deviates slightly from linearity, and has sigmoidal aspects. Additionally, we cannot discount minor changes in tooth growth rate associated with frequent handling of the animals during the water switch period. Although beyond the scope of this study, findings such as these will help guide the refinement and modification of forward modeling techniques so that they can encompass a wider array of growth scenarios, such as non-linear maturation and non-constant growth rate.

We also compared the $\delta^{18}O$ and $\delta^{13}C$ values of tooth enamel produced using laser ablation with results produced using conventional H_3PO_4 methods for all *N. cinerea* (Tables 6 and 7). In the case of oxygen, Passey and Cerling (2006) predicted that $^{18}\varepsilon^*_{laser\text{-}H_3PO_4}$ should be −8‰ to −9‰ because laser ablation analyzes bulk enamel, whereas the H_3PO_4 method analyzes CO_3. Our mean $\varepsilon^*_{laser\text{-}H_3PO_4}$ was -5.8 ± 2.0‰, which is less than the predicted value, but similar to measured values for modern samples (Passey and Cerling, 2006). The difference between expected and measured values may be due to incomplete mixing of all oxygen phases during laser ablation. In spite of this, laser ablation is a viable method for analyzing very small samples that would be destroyed with conventional methods and as a method to sequentially sample small continually-growing teeth.

We also calculated the fractionation between carbonate and body water for 3 *N. cinerea* using the values for $\delta^{18}O_{enamel}$ measured with the H_3PO_4 method. $^{18}\varepsilon^*_{enamel\text{-}bw}$ was 27.0 ± 2.1‰ (Table 6), which is similar to the $^{18}\varepsilon^*_{enamel\text{-}bw}$ value of 26.3‰ measured by Bryant et al. (1996). Bryant et al. (1996) produced an estimate for the apparent fractionation between carbonate and PO_4 in enamel of ~9‰. We can apply this fractionation between PO_4 and carbonate to produce an estimate for the fractionation between the PO_4 and body water for the woodrats. The estimate of $^{18}\varepsilon^*_{PO_4\text{-}bw}$ is ~18‰, which is close to the estimate of ~17.8‰ for lab rats by Luz and Kolodny (1985). Thus, the measured fractionation between body water and tooth enamel appears to be similar for small rodents, regardless of the method used to measure $\delta^{18}O_{enamel}$.

We quantified the fractionations between diet, breath CO_2 and enamel bioapatite for ^{13}C, and we compared measured $\delta^{13}C$ values of the carbonate in the enamel measured using laser ablation with values measured using the H_3PO_4

method. Carbonates in tooth enamel are generally enriched between 9‰ and 15‰ relative to diet depending on differences in digestive physiology, and breath CO_2 can be enriched or depleted relative to diet depending on diet composition and or differences in digestive physiology (Passey et al., 2005b; Podlesak et al., 2005). The mean $^{13}\varepsilon^*_{\text{enamel-diet}}$ value was 11.0 ± 0.1‰, which is within the expected range and close to that measured for voles (Passey et al., 2005b). However, it is slightly higher than the 9.7 ± 0.6‰ measured for laboratory rats (Ambrose and Norr, 1993) and the 9.3 ± 1.4‰ measured for mice (Tieszen and Fagre, 1993). These slight differences may be due to small differences in digestive physiology combined with the difference between bone bioapatite and enamel bioapatite (Passey et al., 2005b). Woodrats and voles are more herbivorous than lab rats and mice, and bone bioapatite was sampled from the lab rats and mice, and enamel bioapatite was sampled from the woodrats and voles.

We also would expect similar fractionations between diet and breath, and enamel and breath for woodrats, voles and mice. $\delta^{13}C$ of the breath samples was consistent across all woodrats and $^{13}\varepsilon^*_{\text{breath-diet}}$ was -0.8 ± 0.5‰ (Table 7). The range in values was similar to values observed in mice (*Mus musculus*) and prairie voles (*Microtus ochrogaster*) (Tieszen and Fagre, 1993; Passey et al., 2005b). Lastly, $^{13}\varepsilon^*_{\text{enamel-breath}}$ was 11.8 ± 0.5‰ which is also similar to the fractionation observed between voles (Passey et al., 2005b). Overall, the fractionation of ^{13}C between diet, breath and enamel by the woodrats is comparable to other small rodents that have similar digestive physiologies.

We also compared $\delta^{13}C$ of the tooth enamel produced with laser ablation with values produced using the H_3PO_4 method. $\delta^{13}C$ values were consistently more depleted when measured with laser ablation and $^{13}\varepsilon^*_{\text{laser-}H_3PO_4}$ was -1.9 ± 0.4‰. Laser ablation also produced slightly greater variation in $\delta^{13}C$ values than did conventional analysis methods (Table 7). Laser ablation may be inherently less precise and accurate than H_3PO_4 analysis, because, unlike the H_3PO_4 method, it does not discriminate among carbon coming from isotopically disparate sources such as organic carbon and inorganic carbon. Nevertheless, the laser ablation method is a viable method of measuring the $\delta^{13}C$ of tooth enamel for small rodents.

4.4. Summary and conclusions

We present the results from a study designed to quantify the relationships between δ_{dw} and δ_{bw} and between δ_{bw} and δ values of multiple tissues for a small rodent. Overall, δ_{dw} had a strong influence on δ_{bw}, and on the δ values of hair and tooth enamel. Drinking water was responsible for 56% of the oxygen atoms and 71% of the hydrogen atoms in the body water of the *N. cinerea*. Food was responsible for the remaining 29% of the hydrogen atoms, and food and molecular O_2 were responsible for 15% and 30% of the remaining oxygen atoms in the body water of the woodrats, respectively.

The turnover of the body water was rapid and had nearly reached isotopic equilibrium 2 weeks after a change in drinking water. We measured the change in δ_{bw} by collecting breath and blood samples. Oxygen in breath CO_2 and the body water were in equilibrium. Breath samples are a non-invasive method of measuring the $\delta^{18}O$ of the body water.

The change in drinking water was also recorded in the hair samples. Drinking water was responsible for 45% of the oxygen and 25% of the hydrogen in the hair of the woodrats. A multiple-pool body water model robustly estimated the δ value of the hair. The change in drinking water was also recorded in the incisors of the woodrats. We used laser ablation to sequentially sample the incisors from 3 of the woodrats and forward modeling adequately estimated $\delta^{18}O$ of the enamel.

The controlled conditions of this experiment permitted us to compare published body water models that predict δ_{bw} values based on δ_{dw} values. A regression model between δ_{dw} and δ_{bw} for lab rats and a model by Gretebeck et al. (1997) accurately estimated δ_{bw} values. A model based on the Kohn (1996) model and customized for the woodrats also reliably estimated δ_{bw} for the woodrats.

In conclusion, the isotopic composition of animal tissues is strongly correlated with local precipitation and as a result, can be used to identify location of origin for samples and to reconstruct climate. However, animals routinely change locations and routinely exploit new resources as they become available. Changes in location and/or change in resource use may influence δ_{bw} and subsequently δ_t. Laboratory experiments in which the isotopic composition of the drinking water and food fed to animal is controlled will increase the ability to use animals' tissues as a tool to identify location of origin and to reconstruct climate.

ACKNOWLEDGMENTS

We thank the members of the Dearing lab that assisted in the care and maintenance of the woodrats and we thank Christy Turnbull for assisting with the blood collection. We also thank Lesley Chesson for prepping and analyzing many of the samples and we thank Mike Lott and Craig Cook of the SIRFER facility at the University of Utah for help in the analysis and interpretation of the stable isotope data. Financial support was provided by NSF to D. Dearing (NSF IBN 0236402) and by IsoForensics. Institutional Animal Care and Use Committee (protocol number 04-02012).

REFERENCES

Ambrose S. H. and Norr L. (1993) Carbon isotope evidence for routing of dietary protein to bone collagen, and whole diet to bone apatite carbonate: purified diet growth experiments. In *Prehistoric Human Bone Archaeology at the Molecular Level* (eds. G. Lambert and G. Grupe). Springer-Verlag, pp. 1–37.

Ayliffe L. and Chivas A. R. (1990) Oxygen isotope composition of the bone phosphate of Australian kangaroos: potential as a paleoenvironmental recorder. *Geochimica et Cosmochimica Acta* **54**, 2603–2609.

Ayliffe L. K., Cerling T. E., Robinson T., West A. G., Sponheimer M., Passey B. H., Hammer J., Roeder B., Dearing M. D. and Ehleringer J. R. (2004) Turnover of carbon isotopes in tail hair and breath CO_2 of horses fed an isotopically varied diet. *Oecologia* **139**, 11–22.

Bowen G. J., Chesson L. A., Nielson K., Cerling T. E. and Ehleringer J. R. (2005a) Treatment methods for the determination of δ^2H and $\delta^{18}O$ of hair keratin by continuous-flow isotope ratio mass spectrometry. *Rapid Communications in Mass Spectrometry* **19**(17), 2371–2378.

Bowen G. J. and Revenaugh J. (2003) Interpolating the isotopic composition of modern meteoric precipitation. *Water Resources Research* **39**(10), 1299.

Bowen G. J., Wassenaar L. I. and Hobson K. A. (2005b) Global application of stable hydrogen and oxygen isotopes to wildlife forensics. *Oecologia* **143**(3), 337–348.

Bryant J. D. and Froelich P. N. (1995) A model of oxygen isotope fractionation in body water of large mammals. *Geochimica et Cosmochimica Acta* **59**(21), 4523–4537.

Bryant J. D., Koch P. L., Froelich P. N., Showers W. J. and Genna B. J. (1996) Oxygen isotope partitioning between phosphate and carbonate in mammalian apatite. *Geochimica et Cosmochimica Acta* **60**, 5145–5148.

Cerling T. E., Ayliffe L. K., Dearing D. M., Ehleringer J. R., Passey B. H., Podlesak D. W., Torregrossa A.-M. and West A. G. (2007) Determining biological tissue turnover using stable isotopes: the reaction progress variable. *Oecologia* **151**, 175–189.

Dansgaard W. (1964) Stable isotopes in precipitation. *Tellus* **16**, 436–467.

Fricke H. C., Clyde W. C. and O'Neil J. R. (1998) Intra-tooth variations in $\delta^{18}O$ (PO_4) of mammalian tooth enamel as a record of seasonal variations in continental climate variables. *Geochimica et Cosmochimica Acta* **62**, 1839–1859.

Fricke H. C. and O'Neil J. R. (1996) Inter- and intra-tooth variation in the oxygen isotope composition of mammalian tooth enamel phosphate: implications for paleoclimatological and paleobioligical research. *Palaeogeography Palaeoclimatology Palaeoecology* **126**, 91–99.

Gretebeck R. J., Schoeller D. E., Socki R. A., Davis-Street J., Gibson E. K., Schulz L. O. and Lane H. W. (1997) Adaptation of the doubly labeled water method for subjects consuming isotopically enriched water. *Journal of Applied Physiology* **82**(2), 563–570.

Hobson K. A. (2005) Stable isotopes and the determination of avian migratory connectivity and seasonal interactions. *The Auk* **122**(4), 1037–1048.

Hobson K. A., Atwell L. and Wassenaar L. I. (1999) Influence of drinking water and diet on the stable-hydrogen isotope ratios of animal tissues. *Proceedings of the National Academy of Sciences of the United States of America* **96**, 8003–8006.

Hobson K. A. and Wassenaar L. I. (1997) Linking breeding and wintering grounds of neotropical migrant songbirds using stable hydrogen isotopic analysis of feathers. *Oecologia* **109**, 142–148.

Hoppe K. A. (2006) Correlation between the oxygen isotope ratio of North American bison teeth and local waters: implication for paleoclimatic reconstructions. *Earth and Planetary Science Letters* **244**, 408–417.

Hoppe K. A., Amundson M., Vavra M., McClaran M. P. and Anderson D. L. (2004) Isotope analyses of equid teeth from modern North American feral horses: implications for paleoenvironmental reconstructions. *Palaeogeography Palaeoclimatology Palaeoecology* **203**, 299–311.

Horita J. and Wesolowski D. J. (1994) Liquid–vapor fractionation of oxygen and hydrogen isotopes of water from the freezing to the critical temperature. *Geochimica et Cosmochimica Acta* **58**(16), 3425–3437.

Kohn M. J. (1996) Predicting animal $\delta^{18}O$: accounting for diet and physiological adaptation. *Geochimica et Cosmochimica Acta* **60**(23), 4811–4829.

Kreuzer-Martin H. W., Ehleringer J. R. and Hegg E. L. (2005) Oxygen isotopes indicate most intracellular water in log-phase *Escherichia coli* is derived from metabolism. *Proceedings of the National Academy of Sciences of the United States of America* **102**, 17337–17341.

Kreuzer-Martin H. W., Lott M. J., Dorigan J. and Ehleringer J. R. (2003) Microbe forensics: oxygen and hydrogen stable isotope ratios in *Bacillus subtilis* cells and spores. *Proceedings of the National Academy of Sciences of the United States of America* **100**(3), 815–819.

Kreuzer-Martin H. W., Lott M. J., Ehleringer J. R. and Hegg E. L. (2006) Metabolic processes account for the majority of the intracellular water in log-phase *Escherichia coli* as revealed by hydrogen isotopes. *Biochemistry* **45**, 13622–13630.

Longinelli A. and Padalino A. P. (1980) Oxygen isotopic composition of water from mammal blood: first results. *European Journal of Mass Spectrometry in Biochemical, Medicine and Environmental Research* **1**(3), 135–139.

Lott C. A. and Smith J. P. (2006) A geographic-information-system approach to estimating the origin of migratory raptors in North America using stable hydrogen isotope ratios in feathers. *The Auk* **123**(3), 822–835.

Luz B. and Kolodny Y. (1985) Oxygen isotope variations in phosphate of biogenic apatites, IV. Mammal teeth and bones. *Earth and Planetary Science Letters* **75**, 29–36.

Luz B., Kolodny Y. and Horowitz M. (1984) Fractionation of oxygen isotopes between mammalian bone-phosphate and environmental drinking water. *Geochimica et Cosmochimica Acta* **48**, 1689–1693.

McKechnie A. E., Wolf B. O. and Martinez del Rio C. (2004) Deuterium stable isotope ratios as tracers of water resource use: an experimental test with rock doves. *Oecologia* **140**, 191–200.

McLister J. D., Sorenson J. S. and Dearing M. D. (2004) Effects of consumption of juniper (*Juniperus monosperma*) on cost of thermoregulation in the woodrats *Neotoma albigula* and *Neotoma stephensi* at different acclimation temperatures. *Physiological and Biochemical Zoology* **77**(8), 305–312.

Nagy K. A., Girard I. A. and Brown T. K. (1999) Energetics of free-ranging mammals, reptiles, and birds. *Annual Review of Nutrition* **19**, 247–277.

Passey B. H. and Cerling T. E. (2002) Tooth enamel mineralization in ungulates: implications for recovering a primary isotopic time-series. *Geochimica et Cosmochimica Acta* **66**(18), 3225–3234.

Passey B. H. and Cerling T. E. (2006) In situ stable isotope analysis ($\delta^{13}C$, $\delta^{18}O$) of very small teeth using laser ablation GC/IRMS. *Chemical Geology* **235**, 238–249.

Passey B. H., Cerling T. E., Schuster G. T., Robinson T. F., Roeder B. L. and Krueger S. K. (2005a) Inverse methods for estimating primary input signals from time-averaged isotope profiles. *Geochimica et Cosmochimica Acta* **69**(16), 4101–4116.

Passey B. H., Robinson T. F., Ayliffe L. K., Cerling T. E., Sponheimer M., Dearing D. M., Roeder B. L. and Ehleringer J. R. (2005b) Carbon isotope fractionation between diet, breath CO_2, and bioapatite in different mammals. *Journal of Archaeological Science* **32**, 1459–1470.

Pflug K. P., Schuster K. D., Pichotka J. P. and Förstel H. (1979) *Fractionation Effects of Oxygen Isotopes in Mammals*. Academic Press.

Podlesak D. W. and McWilliams S. R. (2006) Metabolic routing of dietary nutrients in birds: effects of diet quality and macronutrient composition revealed using stable isotopes. *Physiological and Biochemical Zoology* **79**(3), 534–549.

Podlesak D. W., McWilliams S. R. and Hatch K. A. (2005) Stable isotopes in breath, blood, feces and feathers can indicate intra-

individual changes in the diet of migratory songbirds. *Oecologia* **142**, 501–510.

Ritz P., Cole T. J., Davies P. S., Goldberg G. R. and Coward W. A. (1996) Interactions between ^{2}H and ^{18}O natural abundance variations and DLW measurements of energy expenditure. *American Journal of Physiology: Endocrinology and Metabolism* **271**(34), E302–E308.

Schoeller D. E., Leitch C. A. and Brown C. (1986a) Doubly labeled water method: in vivo oxygen and hydrogen isotope fractionation. *American Journal of Physiology* **251**, R1137–R1143.

Schoeller D. E., Minagawa M., Slater R. and Kaplan I. R. (1986b) Stable isotopes of carbon, nitrogen and hydrogen in the contemporary North American human food web. *Ecology of Food and Nutrition* **18**, 159–170.

Sharp Z. D., Atudorei V., Panarello H. O., Fernández J. and Douthitt C. (2003) Hydrogen isotope systematics of hair: archeological and forensic applications. *Journal of Archaeological Science* **30**, 1709–1716.

Thompson R. C. (1953) Studies of metabolic turnover with tritium as a tracer. II. Gross studies on the rat. *Journal of Biological Chemistry* **200**, 731–743.

Tieszen L. L. and Fagre T. (1993) Effect of diet quality and composition on the isotopic composition of respiratory CO_2, bone collagen, bioapatite, and soft tissues. In *Prehistoric Human Bone Archaeology at the Molecular Level* (eds. J. B. Lambert and G. Grupe). Springer-Verlag, pp. 120–155.

Wolf B. O. and Martinez del Rio C. M. (2003) How important are columnar cacti as sources of water and nutrients for desert consumers? A review. *Isotopes in Environmental and Health Studies* **39**(1), 53–67.

Zanconato S., Cooper D. M., Armon Y. and Epstein S. (1992) Effect of increased metabolic rate on oxygen fractionation. *Respiration Physiology*, 319–327.

Associate editor: Juske Horita